

Arctic, Antarctic and Alpine Research, Vol. 34, No. 4, 2002, pp. 103-114

**Sediment Inclusions in Alaskan Coastal Sea Ice: Spatial Distribution, Interannual  
Variability and Entrainment Requirements**

*Aaron P. Stierle and Hajo Eicken\**

Geophysical Institute, University of Alaska Fairbanks, P.O. Box 757320, Fairbanks, Alaska  
99775-7320, U.S.A.

\*Corresponding author.

*E-mail address:* hajo.eicken@gi.alaska.edu

## Abstract

We investigated the spatial characteristics of sedimentary inclusions and elucidated processes controlling their spatial and temporal variability in the fast ice cover of the shallow-marine environment of Elson Lagoon near Barrow, Alaska. This was accomplished by examining the frazil ice layer of sea-ice cores representing the 1998, 1999, and 2000 fall freeze-up periods and comparing the results with a sediment resuspension model. Sediments occur exclusively as aggregates of clay to fine-silt sized particles that were confined to brine inclusions in the frazil ice. The average cross-sectional area of these aggregates is positively correlated with sediment concentration of the frazil ice ( $R^2 = 0.82$ ,  $P < 0.01$ ). The minimum distance between neighboring aggregates (nearest-neighbor distance) is negatively correlated with sediment concentration ( $R^2 = 0.78$ ,  $P < 0.01$ ). However, little correlation exists between the number of aggregates and sediment concentration. Sediment concentrations ranged from 24 to 1470 mg L<sup>-1</sup> and sediment loads ranged from 2 g m<sup>-2</sup> to 384 g m<sup>-2</sup>, with 1998 and 2000 sediment loads being one to two orders of magnitude smaller than 1999 sediment loads. Similarly, the potential for bottom-sediment resuspension was greater in 1999 than in 1998 and 2000 by more than a factor of two. Resuspension potential is controlled spatially by the local bathymetry and interannually by wind velocity and fetch. At submeter scales, increases in bottom sediment resuspension result in greater sea ice sediment concentrations, larger aggregates and smaller nearest-neighbor distances.

## **Introduction**

Recently, fluctuations in the thickness and areal extent of sea ice and rates of coastal erosion have been observed in the Arctic (Are, 1998; Rothrock et al., 1999; Serreze et al., 2000). These observations have stimulated interest in understanding the natural variability exhibited by the Arctic environment. One particular area of interest is the transport of sediment by sea ice. While sediment-laden sea ice has been documented for well over a century, the mechanisms responsible for the variability in the sediment content of sea ice are poorly understood. Furthermore, the effects of this variability on the properties of the sea-ice cover are not well known. Without a clear understanding of the natural variability in the sediment content of Arctic sea ice, it will be difficult to understand sediment entrainment mechanisms and the effects of sediment inclusions on sea-ice properties.

### *Distribution of Sediment in Sea Ice*

Recent studies suggest that significant natural variability exists in the sediment content of Arctic sea ice (Reimnitz and Kempema, 1987; Clark, 1990; Nürnberg et al., 1994; Reimnitz et al., 1994; Tucker et al., 1999). Satellite observations show a distinct patchiness to the greater-than-meter-scale distribution of sediments in sea ice, while shipboard observations reveal a similar pattern down to the centimeter scale (Nürnberg et al., 1994; Eicken et al., 2000a). Nevertheless, these observations are spotty due to inclement weather and logistical costs and tend to undersample the spatial distribution of sedimentary inclusions. Satellite observations examine only the upper 10 cm of the ice cover at most, even though relatively high sediment concentrations are frequently found deeper in the ice cover (e.g., Osterkamp and Gosink, 1984; Eicken et al., 1997). Neither satellite nor shipboard observations can resolve the subcentimeter-scale spatial distribution of sediments arising from the abundance of micrometer-sized particles and brine inclusions in which the particles appear to reside (Osterkamp and Gosink, 1984; Nürnberg et al., 1994; Perovich and Gow, 1996).

### *Effects of Entrained Sediment on Sea-Ice Properties*

Incorporated sediment may significantly affect properties of the sea-ice cover and processes operating therein. Reductions in both surface albedo and shortwave radiation transmission through the ice cover are caused by entrained sedimentary particles (Light et al., 1998). These reductions are dependent on the size of sediment inclusions (among other factors), which may differ from the particle size of the entrained material. The reduced albedo of sediment-laden sea ice is thought to enhance summer melting and could decrease the areal extent and thickness of the ice cover (Ledley and Pfirman, 1997), potentially threatening polar ecosystems and altering global climate (Intergovernmental Panel on Climate Change, 1990; Tynan and DeMaster, 1997). Reduced shortwave radiation transmission may also significantly diminish total primary productivity underneath and within the ice cover (Horner and Schrader, 1985; Henley and

Dunton, 1997). Clay minerals typically comprise a large portion of sediments entrained in sea ice (Nürnberg et al., 1994; Reimnitz et al., 1998) and may transport contaminants and organic matter to the central Arctic Basin and Nordic Seas (Meese et al., 1997; Nies et al., 1999; Naidu et al., 2000). Entrained sediments may promote microbial activity and growth by acting as a source of macro- and micronutrients (Hedges and Keil, 1995; Measures et al., 1999). At the subcentimeter scale, the spatial distribution of sediment could determine the distribution of metabolically active bacteria by localizing nutrient sources.

### *Sediment Entrainment Process*

Numerous mechanisms for the incorporation of sediments into sea ice have been proposed, including eolian deposition, river discharge onto ice, bottom adfreezing, anchor ice formation, and suspension freezing (Darby et al., 1974; Osterkamp and Gosink, 1984). However, Reimnitz et al. (1993) suggest that suspension freezing is likely to be the dominant mechanism. While the processes by which sediment is entrained into the sea-ice cover by suspension freezing are not completely understood, it is hypothesized that meteorological conditions at the time of autumn freeze-up are important parameters (Reimnitz et al., 1993; Sherwood, 2000). Subfreezing air temperatures in conjunction with turbulent mixing of the water column by wind-induced waves and thermohaline processes result in the formation of frazil ice over the entire depth of the ocean mixed layer. Simultaneously, turbulent shear at the ocean-seabed boundary over shallow shelves leads to resuspension of marine sediments. Continued turbulent mixing results in the flocculation of ice crystals and sediment, as well as the formation of ice crystal aggregates. Once the turbulent mixing abates, buoyant frazil ice crystals rise to the sea surface and form a slushy layer. As they rise, the crystals scavenge remaining suspended sedimentary particles from the water column. At any time, if an ice crystal becomes negatively buoyant due to an excess of attached sedimentary particles, the crystal will sink unless an environmental disturbance (turbulence, particle collision, wave, etc.) causes the particles to be dislodged.

Sediment may be redistributed within the ice cover prior to and during solidification. The passage of wave trains through the slushy layer causes sediment particles to settle (Reimnitz and Kempema, 1987) and may redistribute sediment within this layer. Continued subfreezing air temperatures cause ice formation in the interstices of the slushy layer (congelation). During congelation, the sediment inclusions may be excluded from the ice crystal lattice and aggregated in the remaining brine inclusions (Osterkamp and Gosink, 1984). Congelation experiments in the laboratory suggest that some sediment may also be redistributed in, or lost from, the frazil layer ahead of the freeze front (Clayton et al., 1990).

### *Sediment Sources*

Shallow shelf regions surrounding the deep basins of the Arctic Ocean may serve as the source for most, if not all, of the sediment incorporated into the Arctic sea-ice cover. Provenance studies suggest that the shallow shelves of the Laptev and Kara Seas contribute most of the

sediment seen in Arctic sea ice, and those of the East Siberian and Beaufort Seas appear to be minor source areas (Reimnitz et al., 1993; Pfirman et al., 1997; Eicken et al., 2000a). These shallow shelf regions, which are often ice-free at the end of the summer melt season, are frequented by intense storm systems around the time of autumn freeze-up. The storms provide favorable meteorological conditions for both sediment resuspension and formation of significant frazil ice, and we might expect that the total amount of sediment incorporated into the ice corresponds with meteorological conditions existing during freeze-up.

#### *Linking the Spatial Distribution of Sediment and the Freeze-Up Environment*

In light of potential impacts of sedimentary inclusions on the physical, chemical and biological properties of the Arctic sea-ice cover, it is surprising that so little research has focussed on the subcentimeter-scale spatial distribution of sediments within the ice cover. To date, few studies have related the milli- to micrometer-scale distribution of entrained sediments to sediment concentration and ultimately to large-scale environmental conditions that control sediment entrainment and ice growth processes. In this study, we have attempted to bridge the gap between the small-scale distribution of sediments in sea ice and large-scale environmental conditions.

We determined the relationship between environmental conditions and the subcentimeter-scale spatial distribution of sediment inclusions through a three-part process. First, we linked the small-scale spatial distribution of sedimentary inclusions to sea ice type and large-scale distribution of sediment content by examining samples of the seasonal sea ice cover near Barrow, Alaska, formed during the autumn 1998, 1999, and 2000 freeze-up events. Sediment content was determined using the conventional melt/filter method, while the spatial distribution of sediments was examined using a new image-based method. Second, we employed a sediment resuspension model (after Booth et al., 2000) to examine the relationship between meteorological conditions present during freeze-up and the large-scale spatial and temporal variability of sedimentary inclusions resulting from sediment entrainment. Finally, we linked the environmental conditions prevailing during autumn freeze-up events and the resulting small-scale spatial distribution of sediments within the sea-ice cover.

## Study Site, Materials and Methods

### *Study Site*

The study area is located in the far western Elson Lagoon, 13 km northeast of Barrow, Alaska (Fig. 1). The lagoon is bounded on the northwest and northeast by barrier islands that rise 2 to 3 m a.s.l., while the North Slope of Alaska forms the southwest and southeast coastlines. The lagoon averages 7 km wide and 56 km long and is less than 4 m deep. The barrier islands are composed of gravel. The lagoon floor is composed primarily of unconsolidated muddy sediments, but exposed cobbles have been observed near Eluitkak Pass where the narrow passage enhances current velocities (Reimnitz, pers. comm., Sept. 2001). The grain size of bottom sediments remains relatively constant from year to year due to a lack of terrestrial (no large riverine sources) and marine (barrier islands inhibit sediment input) sources. Sea ice in Elson Lagoon is almost exclusively first-year ice. All ice that forms in the lagoon melts in situ the following summer. Furthermore, the barrier islands inhibit the movement of multiyear ice into the lagoon from the Arctic Ocean. The tidal range in the lagoon is less than 16 cm.

### *Sea Ice Texture and the Spatial and Temporal Analysis of Sea Ice Sediment Inclusions*

Sea-ice cores were extracted from the continuous ice cover of western Elson Lagoon on 14 March 1999, 9 May 2000, and 3 April 2001. A total of 11 cores were collected, two at station 1 in 1999, two each from the stations 1 through 4 in 2000 and one from station 1 in 2001 (Fig. 1, Table 1). The 1999 cores penetrated the full thickness of the ice cover, while those taken in 2000 and 2001 only penetrated the thickness of the sediment-laden layer. These sea-ice cores were representative of the ice types and sediment load found at each location. During the 1999 sampling period air temperatures were  $-30$  to  $-40^{\circ}\text{C}$ , and ice-surface temperatures were  $-15$  to  $-20^{\circ}\text{C}$  (Eicken et al., 2000b). During the 2000 sampling period both air and ice temperatures were approximately  $-5^{\circ}\text{C}$ . During the 2001 sampling period air temperatures ranged from  $-15$  to  $-25^{\circ}\text{C}$  and the ice surface temperature was  $-15^{\circ}\text{C}$ .

The ice cores were extracted using a 10-cm-diameter CRREL-type fiberglass-barrel auger. After extraction, a replicate core from each site (excepting the single core collected in 2001) was maintained at approximately  $-15^{\circ}\text{C}$  until processed for microscopic and macroscopic examination at the University of Alaska Fairbanks. The other cores (including the core from 2001) were cut into 5 to 10 cm segments on site based primarily on depth. Those parts of the cores that appeared to have high sediment concentrations were cut into 5 cm segments for greater resolution. The segments were melted and the melt water from each segment was filtered through a  $1.0\text{-}\mu\text{m}$  A/E glass fiber filter (Gelman Sciences) to collect the entrained sediment. The filtered sediment samples were weighed after they were dried overnight at  $50^{\circ}\text{C}$ .

Two different types of sea-ice samples were prepared from the intact cores for microscopic and macroscopic examination. Horizontal "thick" sections ( $2\text{ cm} \times 2\text{ cm} \times 5\text{-}6\text{ mm}$  thick) for

microscopic examination were prepared as outlined in Junge et al. (2001). These thick sections were examined under both transmitted and cross-polarized light using a cold-adapted Zeiss Axioskop 2 microscope with a 20× objective connected to a digital camera, with an on-screen magnification of 1025×. The microscopic field of view covered an area of 0.041 mm<sup>2</sup> and had a focal depth of 0.02 mm. Two to four transects, typically 80 microscopic fields long, were conducted across each sample and all fields containing sedimentary inclusions were recorded and analyzed. The total number of fields scanned in each transect was noted. Image analysis consisted of outlining each sedimentary inclusion and determining the length of the minor axis of an inscribed ellipse.

Images were acquired using a MTI DC330E 3CCD color camera and a Scion CG-7 RGB Color PCI frame grabber. This combination produced images with 768 by 576 pixels. Image acquisition, calibration, analysis, and display were performed using NIH Image v. 1.62c (Rasband and Bright, 1995), running on a Macintosh G3 with 128MB RAM.

Vertical thin sections (5 cm × 5 cm × ~0.5 mm thick) for macroscopic examination were processed as described by Eicken and Lange (1991), except for cores 1999-1 and 2000-1, which because of mechanical problems, were microtomed to an approximate final thickness of 1.5 mm. For sedimentary particle analysis, images of the thin sections were acquired using a Canon 28-80mm macro-lens connected to the digital camera setup described above. Illumination was provided by a fluorescent light table. On-screen magnification was 12.3× and each pixel represented a linear dimension of 0.026 mm. Each thin section was imaged in a mosaic format with no overlap between adjacent images, producing nine images per sample on average. The resulting three-channel images were then contrast-enhanced. Image segmentation was achieved using an unsupervised, maximum-likelihood, multi-spectral classification scheme in MultiSpec v. 4.2.00 (<http://dynamo.ecn.purdue.edu/~biehl/MultiSpec/>; running on the Macintosh G3 described above) with the number of classes preset to 15. Presetting the number of classes to 15 resulted in one class that consistently corresponded to sedimentary inclusions.

This method was sensitive to the presence of relatively large air pockets and drained brine pockets that were filled with ice shavings during microtoming. These shaving-filled pockets were often misclassified as sedimentary inclusions by the classification scheme. However, such pockets were easily identified by visual inspection of the thin sections and were removed from the classification output of samples from sites 2000-1 and 2000-2. Shavings were removed from all other samples using compressed air before imaging.

The cross-sectional area of each aggregate and the number of aggregates per cubic millimeter (aggregate number density) were determined from the classification output. The distance between an aggregate and its closest neighboring aggregate (nearest neighbor distance) was measured by performing successive non-linear or morphological filters ("dilations"; neighborhood pixel count = 1, iterations = 1) and counting the number of remaining "particles" after each dilation. Finally, the 'nearest-neighbor test for clustering and regularity' was performed

using the nearest neighbor distances (Swan and Sandilands, 1995). The results of this vertical thin section analysis were grouped for each 10 cm length of core (i.e., 0-10 cm, 10-20 cm, etc.) to facilitate comparison to the gravimetric results derived from 10-cm core segments.

A qualitative assessment of ice stratigraphy was made from images of the thin sections between crossed polarizers acquired with an Olympus D-500L digital camera. Illumination was provided by a fluorescent light table. On-screen magnification was 2.9×

A simple geometric model was used to explore the relationship between the spatial distribution and concentration of sediments in the ice cores. We propose that sediment concentration can be estimated from the mean cross-sectional area and number density of aggregates assuming the following:

- (1) mass density of entrained lithologic particles is uniform,
- (2) aggregates of the particles exhibit a constant porosity,
- (3) aggregates are spherical, and
- (4) there is a random spatial distribution of aggregates within the ice.

The proposed model has the form:

$$S = A \left[ \frac{4\pi}{3} \left( \frac{x}{\pi} \right)^{1.5} \right] y + C \quad (1)$$

where  $S$  is the sediment concentration ( $\text{mg L}^{-1}$ ),  $A$  represents a volume-to-concentration conversion factor ( $\text{mg L}^{-1}$ ),  $x$  is the mean aggregate cross-sectional area ( $\text{mm}^2$ ),  $y$  is the mean aggregate number density ( $\text{mm}^{-3}$ ) and  $C$  represents that portion of the sediment concentration ( $\text{mg L}^{-1}$ ) that is unresolvable with the imaging setup.

### *Modeling Sediment Resuspension*

We employed a simple resuspension model (Booth et al., 2000) for shallow lagoon environments. The model predicts locations within a water body that are likely to experience bottom-sediment resuspension based on surface gravity wave theory. Sediment resuspension is assumed to occur when wind-induced oscillatory wave motion reaches the floor of a water body, regardless of bottom microtopography and sediment characteristics. For this to occur, a critical wavelength ( $L$ ) of  $2d$  (where  $d$  is water depth) must be generated (Pond and Pickard, 1983). The critical wavelength is related to wave period ( $T$ ) by (U.S. Army Corps of Engineers, Coastal Engineering Research Center (CERC), 1984)

$$L = gT^2 / 2\pi, \quad (2)$$

where  $g$  is the acceleration due to gravity ( $9.8 \text{ m s}^{-2}$ ). Assuming a wind duration of 24 h, wave period is related to wind velocity ( $U$ ) and fetch ( $F$ ) by (CERC, 1984)

$$gT / U_A = 0.2857(gF / U_A^2)^{1/3}, \quad (3)$$

where the wind stress factor,  $U_A$ , is related to wind velocity by

$$U_A = 0.71(UR_T)^{1.23}. \quad (4)$$

$R_T$  is a boundary layer stability correction factor and is often taken to equal 1.1 (CERC, 1984). From these equations, a critical wind velocity necessary to suspend bottom sediments is determined. The resuspension potential at a given location is the difference between the actual wind velocity and the critical wind velocity.

The 24-h resultant wind speed, water body morphology, and fetch were the only input parameters. We used meteorological data for Barrow, (National Climatic Data Center, <http://www.ncdc.noaa.gov>) because this station is only 13 km from the study site. The shoreline and bathymetry of Elson Lagoon were digitized from 1:63,360 topographic maps (U. S. Geological Survey, 1955). The fetch was calculated for eight dominant wind directions at every point in a grid with a point spacing of 165 m. Values of resuspension potential were then calculated with a version of the resuspension model adapted in ArcInfo (ESRI, Redlands, CA), a GIS software package.

The model results were compared with satellite images of resuspension patterns as outlined by Booth et al. (2000), with modifications to account for sea ice. Booth et al. found a strong positive correlation between reflectance and turbidity. Increased water turbidity implies an increase in the concentration of suspended sediments. Thus, Booth et al.'s comparison of the resuspension model results with reflectance measurements is an indirect comparison of resuspension potential and the relative sediment concentration in the water column. Advanced Very High Resolution Radiometer (AVHRR) level 1b High Resolution Picture Transmission (HRPT) imagery was collected from the National Oceanic and Atmospheric Administration's Satellite Active Archive (<http://www.saa.noaa.gov/>) for those sea-ice-free days when little or no cloud cover was present over the study area. The images were georeferenced and converted to percent reflectance using TerraScan (SeaSpace Corp., Poway, CA) software with auxiliary parameters outlined in Di and Rundquist (1994). The reflectance of each pixel along a transect across each image was compared in ArcInfo with the modeled estimate of resuspension potential at points corresponding to the pixel centers.

## Results

### *Sea Ice Texture*

Figure 2 shows two images of ice crystals that are representative of all core segments analyzed. The crystals of the uppermost, sediment-laden layers are typical of frazil ice with predominantly small (<10 mm diameter), equant to prismatic shapes and irregular outlines rather than the large, columnar crystals representative of congelation ice growth (Weeks and Ackley, 1986). Below the analyzed core segments, crystals are almost exclusively of the typical vertically elongated (up to >10 cm long) columnar shape with numerous intra- rather than intercrystalline brine inclusions. These observations have been confirmed by detailed microstructural and stratigraphic analyses as part of another study at the same site (Cole, pers. comm., May 2001). There was no evidence of deformation in the core samples nor were there any indications of pancake ice formation, neither from ice textural studies nor from studies of the ice surface, which would have exhibited a corresponding surface of pointy roughness elements and raised edges of individual pancake units.

### *Spatial and Interannual Variability of Sediment Inclusions*

In general the core sediments appear diffusely distributed and fine grained to the unaided eye. There are no regions of excessively large sediment inclusions (except for the 30-40 cm segment of core 1999-1, see below), indications of coarser, platy crystals in the thick and thin sections or undulating layers of sediment, all of which are typical of anchor ice. Therefore, we conclude that the sea ice sampled in all three years resulted primarily from suspension freezing. It is not clear why sediments extend so deep into core 2000-3. One possibility is that the long fetch during freeze-up combined with the relatively deep floor under the site to enhance the depth of frazil ice that accumulated. Another possibility is that ice rafting occurred and doubled the thickness of the ice cover, however the lack of deformation features makes this unlikely.

Sea ice samples from the study area exhibit a patchy distribution of sediment inclusions at different scales (Fig. 3). Microscopic examination reveals that the sediment is concentrated almost exclusively in brine inclusions (primarily brine pockets and the intersections of three or more grains (triple junctions)) rather than in the ice matrix. Gravimetric sediment concentrations range from 24 to 1470 mg L<sup>-1</sup> (mean = 564 mg L<sup>-1</sup> ± 432 mg L<sup>-1</sup> (1σ)), with the lowest concentrations occurring in core 1999-1 and the highest occurring in core 2000-1 (Table 2).

Aggregate number densities, cross-sectional areas and nearest-neighbor distances show a high degree of interannual variability (Table 2). Aggregate number densities span two orders of magnitude from 0.01 to 3.55 mm<sup>-3</sup> (mean = 0.83 mm<sup>-3</sup> ± 0.74 mm<sup>-3</sup>). The aggregate number density is significantly lower ( $P < 0.05$ ) in 1999 (mean = 0.05 mm<sup>-3</sup> ± 0.07 mm<sup>-3</sup>) than in 2000 (mean = 0.99 mm<sup>-3</sup> ± 0.71 mm<sup>-3</sup>). Both aggregate cross-sectional areas and nearest-neighbor distances exhibit a six-fold range of values. Aggregate cross-sectional areas vary from 0.0013 to

0.0084 mm<sup>2</sup>. The 1999 values tend to occupy the lower part of this range, while samples from 2000 cover almost the entire range of values. Nearest-neighbor distances range from 0.33 to 2.33 mm, with core 1999-1 exhibiting distances averaging 2.4 times those found in samples from 2000.

There is also a high degree of intra-core variability in these three spatial descriptors. Individually, the cores show two- to 16-fold differences between the lowest and highest number densities, and two- to six-fold differences between minimum and maximum cross-sectional areas. Nearest-neighbor distances vary by up to a factor of four in each core. Nevertheless, in general inter-core variability (and inter-annual variability) is greater than intra-core variability.

The nearest-neighbor statistic is much less variable, with values falling between 0.54 and 0.92 (Table 2). The nearest-neighbor statistic is significantly lower ( $P < 0.05$ ) in 1999 (mean =  $0.63 \pm 0.09$ ) than in 2000 (mean =  $0.83 \pm 0.07$ ). Swan and Sandilands (1995) indicate that the nearest-neighbor statistic can vary from 0 (highly clustered with all points lying on essentially the same location) to 2.15 (uniformly spaced points), with a random distribution represented by intermediate values. Thus, collectively, the samples appear to exhibit a random spatial distribution of particles, but with some tendency toward clustering. More specifically, samples from 1999 appear to have a more clustered spatial distribution than samples from 2000.

In all further analyses of the macroscopic data, the 30-40 cm segment of core 1999-1 and the 20-30 cm segment of core 2000-2 have been excluded. The first segment has been excluded because the mean cross-sectional area of aggregates is three times greater than that of other segments with similar sediment concentrations (Table 2). Visual inspection of this segment revealed atypically large and elongated sediment inclusions. The mechanism responsible for including such unusual aggregates into the frazil ice layer is unknown, but the incorporation of anchor ice is a possibility. The second segment has been excluded, because the mean aggregate number density for this segment appears to be an outlier (3.7 standard deviations away from the mean). It is unclear why the aggregate number density of this segment is so much greater than that other segments with similar sediment concentrations (Table 2).

Some spatial characteristics are highly correlated with sediment concentration. Nearest-neighbor distance and aggregate cross-sectional area correlate with sediment concentration ( $R^2 = 0.78$  and  $R^2 = 0.82$ , respectively,  $P < 0.01$ ; Figure 4). However, aggregate number density is poorly correlated with sediment concentration ( $R^2 = 0.09$ ,  $P > 0.05$ ).

Figure 5 illustrates the relationship between the cross-sectional area and aggregate number density and the measured sediment concentration. The best-fit geometric model ( $R^2 = 0.61$ ,  $P < 0.01$ ) is:

$$\text{Sediment concentration (mg L}^{-1}\text{)} = 2.8 \times 10^6 \text{ mg L}^{-1} \times [4/3 \times \pi \times (\text{cross-sectional area}/\pi)^{1.5}] \times (\text{aggregate number density}) + 260 \text{ mg L}^{-1}$$

The value of  $2.8 \times 10^6 \text{ mg L}^{-1}$  for the volume-to-mass conversion factor compares favorably with a theoretical value (assuming aggregates with 0% porosity) of  $2.94 \times 10^6 \text{ mg L}^{-1}$ .

The results of the microscopic image analysis are shown in Table 2. Seventeen transects were examined from Elson Lagoon ice samples, yielding 103 sedimentary aggregates in 1999 and 90 in 2000. The aggregate number density in the 2000-1 sample is 3.4 times greater than in the 1999-1 sample. The average aggregate width is 3.1 times greater in the 1999-1 sample than in the 2000-1 sample. These trends are similar to trends in number density and cross-sectional area observed macroscopically. Microscopic aggregate number densities are approximately three orders of magnitude larger than those determined using the macroscopic imaging technique. It is likely that much of the difference in number densities between the two techniques is due to the 83-fold difference in magnifications used.

### *Modeling Sediment Resuspension*

The results from the assessment of the resuspension model's applicability to Elson Lagoon are shown in Figure 6. According to Booth et al. (2000), resuspension potentials of zero or less represent areas where no sediment resuspension is predicted to occur, while positive resuspension potentials suggest that resuspension of bottom sediments is taking place. The resuspension potentials of zero or less shown in Figure 6 correspond to low reflectance values (<5.8%). Resuspension potentials greater than 5 correspond to higher reflectance values (>5.8%). As previously stated, higher reflectance values imply increased suspended sediment concentrations. Furthermore, as resuspension potentials increase beyond that necessary to initiate the resuspension of sediments the implication is that greater and greater amounts of sediment will be suspended. Thus, as resuspension potential increases, one would expect an increase in the concentration of suspended sediments and consequently an increase in reflectance values. Good agreement between the predicted onset of sediment resuspension and increased reflectance from the water suggests that the resuspension model is applicable to Elson Lagoon in the absence of sea ice.

Predicted bottom-sediment resuspension potentials for the fall freeze-up periods corresponding to the spring 1999, 2000 and 2001 sampling seasons are shown in Figure 7. Resuspension potential values and corresponding sediment loads for specific sampling sites are listed in Table 3. The fall 1998 and 2000 freeze-up events were characterized by relatively light winds and low resuspension potentials (less than +8) over much of the study area. During the fall 1999 freeze-up event, relatively high wind stress and a long fetch resulted in resuspension potentials in excess of +10 over most of the study area. The predicted resuspension potential corresponding to site 1 (cores 1999-1 and 2000-1) was 2.3 times greater in 1999 than in 1998. The model predicted no resuspension at site 1 in 2000. Trends in sediment load between the three years were similar, with core 2000-1 having an average sediment load six times greater than core 1999-1 and 174 times greater than core 2001-1.



## Discussion

The multi-scale approach employed in this study yielded a number of significant results. Significant natural variability exists both spatially and temporally within the sea ice cover. Meteorological conditions at the time of freeze-up are important factors determining bulk sediment content and the spatial distribution of sediments within the sea-ice cover. Processes responsible for sediment entrainment and sea ice formation in Elson Lagoon are similar and depend on only a few environmental parameters, namely water depth, fetch, and wind velocity (the latter averaged over 24 h).

### *Potential Sources of Error - Image Analysis*

Several factors may have influenced the results of the image analysis. First, it should be noted that the method employed to determine nearest-neighbor distances ignores the dimensions of the aggregates. We estimate that this method results in an average error of only 12% (assuming spherical aggregates), which should not significantly affect the findings of this study. Second, the minimum resolution of the macroscopic imaging system (0.026 mm, silt size) may have resulted in the underestimation of aggregate number densities and overestimation of cross-sectional areas and nearest-neighbor distances. On the other hand, highly significant correlations between sediment concentration and cross-sectional area and nearest-neighbor distance together with the continuation of trends from the centimeter to micrometer scale demonstrate that the resolution limitation is not an important source of error. Third, the analysis of images of a finite size introduces a boundary effect that could result in the underestimation of nearest-neighbor distances. However, given the natural variability observed in the samples this error is not deemed important in contrast to other sources of error inherent in our approach. Fourth, the effect of representing volumes (thin sections) as planar surfaces (images) could potentially result in the overestimation of number densities and underestimation of nearest-neighbor distances, especially at higher number densities. A comparison of nearest-neighbor distances with sample thickness (same order of magnitude) together with low number densities (typically  $\leq 1 \text{ mm}^{-3}$ ) suggests that the representation of volumes as planar surfaces does not significantly influence the results of this study. Finally, the results may have been biased by the sampling technique used. The macroscopic analysis of only vertical thin sections from widely spaced cores may have resulted in an inadequate sampling of the horizontal variability at the centimeter scale. Nevertheless, the reproduction of trends in the macroscopic results by the microscopic analysis together with strong correlations between several parameters imply that the above factors did not significantly bias the results of the macroscopic image analysis.

### *Potential Sources of Error - Modeling Sediment Resuspension*

The sediment resuspension model (Booth et al., 2000) we used may have influenced the results of this study. First, the resuspension model does not incorporate tides or intruding mean ocean currents. However, in light of the small tidal amplitude (16 cm) and extensive system of barrier islands surrounding the lagoon, we feel that tides and ocean currents can be ignored. Second, the model does not address the potential for anchor ice formation or ice-bonded sediments. While observations of anchor ice and ice bonding are numerous in other Arctic coastal environments, we are not aware of a working model for the formation of anchor ice or ice-bonded sediments. Considering that the sediments in the lagoon are predominantly fine-grained, it is likely that the potential for anchor ice and ice-bonded sediments is small. Third, the resuspension model does not account for increases in the water-column sediment concentration resulting from wallowing ice floes. Ice wallowing has periodically been observed along the Beaufort Sea coast (Reimnitz, pers. comm., Sept. 2001). However, considering that Elson Lagoon is sheltered by barrier islands and that the lagoon is typically ice free prior to freeze-up, we consider ice wallowing to be an unlikely event in the lagoon. Finally, the model assumes that sediment resuspension occurs when wave motion reaches the bottom of the lagoon. It has been shown that considerable shear stress must be applied to the sediment surface to resuspend sediments (Komar and Miller, 1973; Drake et al., 1980). This source of error is examined in more detail below.

### *Spatial and Temporal Characteristics of Sedimentary Inclusions*

Interactions between frazil ice crystals and sediment particles during freeze-up and congelation determine the location of sedimentary inclusions in the ice cover. Our finding that sedimentary inclusions are restricted to intercrystalline brine inclusions (primarily triple junctions and brine pockets; Figs. 3c, 3d) supports the hypothesis of Osterkamp and Gosink (1984) that the formation and evolution of frazil ice constrains the location of sediments contained in the ice to brine inclusions. Moreover, the clustering described by the nearest-neighbor statistic occurs over the range of micrometers to millimeters, which includes the scale of individual ice crystals. We hypothesize that the tendency toward a clustered spatial distribution of sediment in frazil ice at sub-centimeter scales is primarily due to the exclusion of sediment from ice crystals during their growth and maturation.

Sea-ice sediment concentration controls some spatial characteristics of sedimentary inclusions in the ice cover. As the sediment concentration increases, aggregates grow larger and the minimum distance between aggregates decreases, possibly due to physical aggregation or flocculation (Fig. 4). In addition, the combination of aggregate number density and cross-sectional area explain 61% of the variance in sediment concentration within the frazil layer of first-year sea ice (Fig. 5). The persistence of these correlations from year to year indicates that they are independent of space and time. Therefore, one should be able to reconstruct a first-order

approximation of the spatial characteristics of sedimentary aggregates within the frazil-ice layer of first-year sea ice from measured sediment concentrations.

Sediment concentration is not the primary control on aggregate number density. The poor correlation between sediment concentration and aggregate number density together with the influence of frazil crystals on the spatial distribution of sediment inclusions imply that ice crystals may control the aggregate number density. The irregular outlines of frazil crystals make it unlikely that neighboring crystals in the slushy layer will have parallel boundaries. As the crystals enlarge during congelation, sediments are likely to be concentrated by the encroaching ice into the larger brine inclusions remaining between crystals. Crystal growth may continue until the walls of the brine inclusions encounter the sediment inclusions, at which point incompatibilities in the sediment and ice crystal structures would preclude further ice growth. It follows that the size of sediment inclusions should depend on the amount of sediment trapped between neighboring crystals (sediment concentration), while the number of inclusions should depend on the morphology of neighboring frazil crystals.

The bulk of the entrained sediment is contained in aggregates that are resolvable with the macroscopic setup (minimum cross-sectional area =  $0.0007 \text{ mm}^2$ ) employed here. The estimated unresolvable sediment concentration ( $C$ ) of  $260 \text{ mg L}^{-1}$  is small compared to many of the sediment concentrations observed in this study. Although the number densities observed under the microscope are two orders of magnitude greater than the macroscopic number densities, it appears that the additional aggregates are so small that they account for only a fraction of the sediment content. Good agreement between the theoretical and empirical volume-to-mass conversion factor ( $A$ ) also indicates that much of the entrained sediment occurs as relatively large aggregates. Thus, the automated macroscopic imaging technique appears to be a valid method for analyzing sedimentary inclusions in sea ice as long as the limitations imposed by the relatively low resolution are kept in mind.

### *Modeling Sediment Resuspension*

While the sediment resuspension model predicts the onset of sediment resuspension in Elson Lagoon during the ice-free season reasonably well, the minimum resuspension potential at which resuspension occurs is unclear (Fig. 6). One possible explanation is that the use of high-latitude satellite imagery introduces errors into the percent reflectance calculations. The surface reflectance of water in the visible and near-infrared wavelengths may be enhanced by the low elevation of the sun during the summer at the latitude of Elson Lagoon. Another possible explanation is that the assumption that sediment is resuspended as soon as wave motion interacts with the bottom is incorrect. To test the validity of this assumption, we estimated the unidirectional current velocity at the sediment-water interface and the range of grain sizes that would be suspended during the 1998, 1999 and 2000 freeze-up events following the approach of Sharma et al. (1972). This model predicts that current velocities near the sediment-water

interface are insufficient to resuspend sediment at resuspension potentials of less than  $\sim+4$ . The model predicts that fine-grained sediment (mostly silt) would be suspended at all coring locations during the 1998 and 1999 freeze-up periods, but not during the 2000 freeze-up period. While these results agree with the resuspension model predictions, the discrepancy in the minimum resuspension potential ( $+4$  vs.  $0$ ) needs a more rigorous assessment. A resuspension potential of  $+4$  corresponds to a bottom shear stress of  $\sim 0.5 \text{ Nm}^{-2}$  and a critical shear velocity of  $\sim 2 \text{ cm s}^{-1}$  (calculated from equations in Komar and Miller (1973)). A critical shear velocity of  $\sim 2 \text{ cm s}^{-1}$  is close to that estimated by Drake et al. (1980) of  $1.3 \text{ cm s}^{-1}$  for fine-grained sediments in Norton Sound. Thus, it appears that a minimum resuspension potential of  $+4$  is required to resuspend bottom sediments in Elson Lagoon.

The success of the resuspension model in predicting the resuspension of bottom sediment based solely on the interaction of wind-induced waves with the sea floor indicates that sediment resuspension in Elson Lagoon occurs primarily in response to the passage of storm systems. The resuspension model predicts that the largest waves and greatest resuspension potentials occur when storms generate strong winds that blow over long fetches of relatively shallow water. In addition, greater resuspension potentials appear to correlate with enhanced water turbidity (Figure 7). Therefore, the timing and duration of intense storms that generate surface gravity waves capable of inducing significant sediment resuspension through interactions with bottom sediments in Elson Lagoon are critical in determining water-column sediment concentrations.

Environmental conditions during autumn freeze-up events in Elson Lagoon also influence the sea ice sediment load. A qualitative comparison of resuspension potential with the sea ice sediment load reveals that higher resuspension potentials result in greater sediment loads (Fig. 7, Table 3). In addition, of the three model input parameters, only wind velocity and fetch vary from year to year, suggesting that these two parameters are responsible for the interannual differences in the magnitudes of resuspension potential and sediment load. Furthermore, a comparison of the bathymetry of Elson Lagoon with the resuspension potential maps for 1998, 1999 and 2000 shows that the shallower southwestern half of the study area generally exhibits higher resuspension potentials than the deeper northeastern half in any one year (Figs. 1, 8). Thus, higher resuspension potentials and sediment loads correlate with shallower regions and vice versa. The persistence of these correlations from year to year indicates that bathymetry determines the spatial variability of resuspension potential and sediment load. The link between sea-ice sediment concentration and resuspension potential suggests that the meter-scale distribution of sediments in Elson Lagoon sea ice could be estimated by mapping the resuspension potential over a region at the time of freeze-up.

The presence of such large aggregates and relatively high sediment concentrations require that thousands of individual sediment particles be captured by individual frazil crystals. We have estimated from thin section images that the average frazil crystal volume in the 2000 samples is  $\sim 100 \text{ mm}^3$ . In these samples, each frazil crystal has on average  $10^1$  to  $10^2$  aggregates associated

with it. Furthermore, assuming that spherical, silt-size grains (10  $\mu\text{m}$  dia.) comprise the aggregates (also assumed to be spherical), we estimate that the average aggregate contains roughly  $10^2$ - $10^3$  particles. This suggests that each ice crystal entrains on the order of  $10^4$  grains into the ice cover. Each frazil crystal must undergo a minimum of  $10^6$  collisions with suspended sediment particles if one employs a collection efficiency of 0.025 (Smedsrud, 1998). Significantly fewer collisions would be required to reach observed aggregate number densities and sediment concentrations if aggregates of sediment particles, rather than individual sediment particles, were entrained by frazil ice.

### *Environmental Conditions and the Spatial Characteristics of Sediments*

The influence of the freeze-up environment extends beyond the meter-scale distribution of sediment inclusions. Environmental conditions (i.e., bathymetry, fetch, and wind velocity) impact the size and minimum spacing of sediment inclusions by determining the water-column sediment concentration and ultimately the concentration of sediments in the ice cover. Environmental conditions also determine the growth mode (i.e., whether frazil ice or columnar ice forms) of sea ice and thereby the morphology of ice crystals in the water column (Weeks and Ackley, 1986). Thus, the tendency toward a clustered spatial distribution brought about by the presence of frazil crystals is inherited from the freeze-up environment, as well. Given the considerable influence of environmental conditions on the characteristics of sedimentary inclusions, we propose that detailed studies of these characteristics in first-year sea ice can be used to reconstruct the freeze-up environment.

### *Scales of Dominant Processes and Their Implications*

The above discussion highlights the two principal scales on which the dominant processes of sediment entrainment and distribution operate. At larger scales ( $10^0$  to  $10^4$  m), the movement of air over the ocean's surface generates waves that create a turbulent water column. This turbulence may resuspend bottom sediments and, in supercooled water, results in the formation of frazil ice. At smaller scales ( $10^{-6}$  to  $10^{-2}$  m), individual frazil crystals physically collect sediment from the water column and carry it to the surface of the ocean to form a slushy layer. Exposure to subfreezing air temperatures causes the ice crystals to grow and concentrate sediment into select intercrystalline brine inclusions.

The expansive area over which a single storm can cause the entrainment of sediments into sea ice suggests that sediment entrainment can play an important role in coastal sediment dynamics and the transport of pollutants and nutrients. The spatial and temporal variability of sedimentary inclusions in sea ice suggest that there may be similar variability in the amount of pollutants and nutrients present in the ice cover and ultimately delivered to the central Arctic

Basin and Nordic Seas. Several sources of nutrients (e.g., river deltas) and pollutants (e.g., radioactive waste dumps) are in close proximity to regions known to contribute large amounts of sediment to the sea ice cover. Given the reactivity between clay minerals and radioactive contaminants and organic matter, it is likely that sea ice formed during times of greater sediment resuspension could contain higher levels of radioactive contaminants and organic matter than ice formed under relatively calm conditions. Higher concentrations of organic matter may in turn result in greater bacterial abundance. Increased microbial respiration could enhance biogeochemical changes occurring in the ice cover. Thus, environmental conditions during fall freeze-up are likely to affect the chemical properties of the sea-ice cover.

### *Need for Future Research*

While the sediment resuspension model appears suitable for Elson Lagoon, further study is needed to assess its applicability to the shallow shelves of the Arctic Ocean. Specifically, the sensitivity of the model to variations in the areal extent and depth of shallow environments must be determined. Also, the impact of variations in the cohesiveness and grain size of sediments and of tidal and ocean currents on model results needs to be assessed. Nevertheless, similarities between Elson Lagoon and the open ocean, together with the lagoon's excellent accessibility make studies of sediment entrainment into sea ice in the lagoon a potential surrogate for more expensive and logistically challenging transoceanic cruises to study similar characteristics.

More research also needs to be done on the impact of wave action and the migration of a freeze front on the spatial distribution of sediments. Both wave action and freeze-front migration may result in the downward migration and loss of sediments from the slushy layer prior to the solidification of this layer. The potential for the entrainment of sediments into the ice cover by anchor ice also needs to be researched further. Any of these three mechanisms could be responsible for some of the unexplained variability in the spatial distribution of sediments.

## Conclusions

In sea ice from Elson Lagoon, sediment inclusions are typically aggregates of clay- and silt-sized particles and occur exclusively in intercrystalline brine inclusions. Sediment concentration is positively correlated with mean aggregate cross-sectional area, suggesting that physical or chemical aggregation occurs within the ice cover. Sediment concentration is negatively correlated with mean nearest-neighbor distance. The number density of sediment inclusions is most likely controlled by crystal morphology rather than the sediment concentration. The sedimentary inclusions exhibit a somewhat clustered spatial distribution within the ice due to the exclusion of sediment from growing ice crystals.

A simple sediment resuspension model is capable of predicting the onset of sediment resuspension in Elson Lagoon based on a limited number of environmental parameters, namely water depth, wind velocity and fetch. The potential for resuspension appears to be controlled spatially by the local water depth and interannually by the wind velocity and fetch. The resuspension model also qualitatively predicts the spatial distribution of sediment load in the ice cover for a particular year as well as interannual variability in the sediment load, based on the values of the above parameters from the previous fall freeze-up period.

Together, the findings of this study imply that environmental conditions at the time of fall freeze-up not only influence the sediment load of sea ice, but also the spatial distribution of sedimentary inclusions in the ice cover. Therefore, the freeze-up environment may affect the natural variability of the properties of and processes acting in the sea ice environment that are dependent on the presence of sediments. By modeling the freeze-up environment over the full range of naturally occurring conditions, it should be possible to estimate the range of natural variability exhibited by these properties and processes.

### *Acknowledgments*

Funding for this project came from NSF (LEn) Grant OPP-9817738. Additional NSF support through the Barrow Arctic Science Consortium, particularly the help of D. Ramey, allowed field work to go smoothly. Further help from C. Krembs, K. Junge, K. Frey, A. Mahoney, and K. Engle is gratefully acknowledged. Comments by E. Reimnitz, C. Sherwood, W. B. Tucker and an anonymous reviewer helped improve the manuscript.

## References Cited

- Are, F. E., 1998: The contribution of shore thermoabrasion to the Laptev Sea sediment balance. In Lewkowicz, A. G. and Allard, M. (eds.), *Proceedings 7th International Conference on Permafrost, Yellowknife*. Sainte-Foy, Québec: Université Laval, Centre d'études nordiques, 25-30.
- Booth, J. G., Miller, R. L., McKee, B. A., and Leathers, R. A., 2000: Wind-induced bottom sediment resuspension in a microtidal coastal environment. *Continental Shelf Research*, 20: 785-806.
- Clark, D. L., 1990: Arctic Ocean ice cover; geologic history and climatic significance. In Grantz, A., Johnson, L., and Sweeney, J. F. (eds.), *The Arctic Ocean Region. The Geology of North America, Vol. I*. Boulder: Geological Society of America, 53-62.
- Clayton, J. R., Reimnitz, E., Payne, J. R., and Kempema, E. W., 1990: Effects of advancing freeze fronts on distributions of fine-grained sediment particles in seawater- and freshwater-slush ice slurries. *Journal of Sedimentary Petrology*, 60: 145-151.
- Cole, D. May 2001. Personal communication. CRREL, Hanover, New Hampshire.
- Darby, D. A., Burkle, L. H., and Clark, D. L., 1974: Airborne dust on the Arctic pack ice, its composition and fallout rate. *Earth and Planetary Science Letters*, 24: 166-172.
- Di, L. and Rundquist, D. C., 1994: A one-step algorithm for correction and calibration of AVHRR Level 1b data. *Photogrammetric Engineering & Remote Sensing*, 60: 165-171.
- Drake, D. E., Cacchione, D. A., Muench, R. D., and Nelson, C. H., 1980: Sediment transport in Norton Sound, Alaska. *Marine Geology*, 36: 97-126.
- Eicken, H. and Lange, M. A., 1991: Image analysis of sea-ice thin sections: a step towards automated texture classification. *Annals of Glaciology*, 15: 204-209.
- Eicken, H., Reimnitz, E., Alexandrov, V., Martin, T., Kassens, H., and Viehoff, T., 1997: Sea-ice processes in the Laptev Sea and their importance for sediment export. *Continental Shelf Research*, 17: 205-233.

- Eicken, H., Bock, C., Wittig, R., Miller, H., and Poertner, H-O., 2000b: Magnetic resonance imaging of sea-ice pore fluids: methods and thermal evolution of pore microstructure. *Cold Regions Science and Technology*, 31: 207-225.
- Eicken H., Kolatschek, J., Freitag, J., Lindemann, F., Kassens, H., and Dmitrenko, I., 2000a: A key source area and constraints on entrainment for basin-scale sediment transport by Arctic sea ice. *Geophysical Research Letters*, 27: 1919-1922.
- Hedges, J. I and Keil, R. G., 1995: Sedimentary organic matter preservation: an assessment and speculative synthesis. *Marine Chemistry*, 49: 81-115.
- Henley, W. J. and Dunton, K. H., 1997: Effects of nitrogen supply and continuous darkness on growth and photosynthesis of the arctic kelp *Laminaria solidungula*. *Limnology and Oceanography*, 42: 209-216.
- Horner, R. and Schrader, G. C., 1985: Relative contributions of ice algae, phytoplankton, and benthic microalgae to primary production in nearshore regions of the Beaufort Sea. *Arctic*, 35: 485-503.
- Intergovernmental Panel on Climate Change (IPCC), 1990: *Climate Change: The IPCC Scientific Assessment*. Cambridge: Cambridge University Press. 365 pp.
- Junge, K., Krembs, C., Deming, J., Stierle, A., and Eicken, H., 2001: A microscopic approach to investigate bacteria under in-situ conditions in sea ice samples. *Annals of Glaciology*, 33: 304-310.
- Komar, P. D. and Miller, M. C., 1973: The threshold of sediment movement under oscillatory water waves. *Journal of Sedimentary Petrology*, 43: 1101-1110.
- Ledley, T. S. and Pfirman, S., 1997: The impact of sediment-laden snow and sea ice in the arctic on climate. *Climatic Change*, 37: 641-664.
- Light, B., Eicken, H., Maykut, G. A., and Grenfell, T. C., 1998: The effect of included particulates on the spectral albedo of sea ice. *Journal of Geophysical Research*, 103: 27739-27752.
- Measures, C. I., 1999: The role of entrained sediments in sea ice in the distribution of aluminium and iron in the surface waters of the Arctic Ocean. *Marine Chemistry*, 68: 59-70.

- Meese, D. A., Reimnitz, E., Tucker III, W. B., Gow, A. J., Bischof, J., and Darby, D. 1997. Evidence for Radionuclide Transport by Sea Ice. *The Science of the Total Environment*, 202:267-278.
- Naidu, A. S., Cooper, L. W., Finney, B. P., Macdonald, R. W., Alexander, C., and Semiletov, I. P., 2000: Organic carbon isotope ratios ( $\delta^{13}\text{C}$ ) of Arctic Amerasian Continental shelf sediments. *International Journal of Earth Sciences*, 89: 522-532.
- Nies, H., Harms, I. H., Karcher, M. J., Dethleff, D., and Bahe, C., 1999: Anthropogenic radioactivity in the Arctic Ocean - review of the results from the joint German project. *The Science of the Total Environment*, 237/238: 181-191.
- Nürnberg, D., Wollenburg, I., Dethleff, D., Eicken, H., Kassens, H., Letzig, T., Reimnitz, E., and Thiede, J., 1994: Sediments in Arctic sea ice: implications for entrainment, transport and release. *Marine Geology*, 119: 185-214.
- Osterkamp, T. E. and Gosink, J. P., 1984: Observations and analyses of sediment-laden sea ice. In Barnes, P. W., Schell, D. M., and Reimnitz, E. (eds.), *The Alaskan Beaufort Sea. Ecosystems and Environments*. London: Academic Press, 73-93.
- Perovich, D. K. and Gow, A. J., 1996: A quantitative description of sea ice inclusions. *Journal of Geophysical Research*, 101: 18327-18343.
- Pfirman, S., Colony, R., Nürnberg, D., Eicken, H., and Rigor, I., 1997: Reconstructing the origin and trajectory of drifting arctic sea ice. *Journal of Geophysical Research*, 102: 12575-12586.
- Pond, S. and Pickard, G. L., 1983: *Introductory Dynamical Oceanography*. Boston: Butterworth-Heinemann. 329 pp.
- Rasband W. S. and Bright, D. S., 1995: NIH Image: a public domain image processing program for the Macintosh. *Journal of Microbeam Analysis*, 4: 137-149.
- Reimnitz, E., Sept. 2001: Personal communication. U. S. Geological Survey, Menlo Park, California.
- Reimnitz, E. and Kempema, E. W., 1987: Field observations of slush ice generated during freeze-up in Arctic coastal waters. *Marine Geology*, 77: 219-231.

- Reimnitz, E., McCormick, M., McDougall, K., and Brouwers, E., 1993: Sediment export by ice rafting from a coastal polynya, Arctic Alaska, U.S.A. *Arctic and Alpine Research*, 25: 83-98.
- Reimnitz, E., Dethleff, D., and Nürnberg, D., 1994: Contrasts in Arctic shelf sea-ice regimes and some implications: Beaufort Sea versus Laptev Sea. *Marine Geology*, 119: 215-225.
- Reimnitz, E., McCormick, M., Bischof, J., and Darby, D. A., 1998: Comparing sea-ice sediment load with Beaufort Sea shelf deposits: Is entrainment selective? *Journal of Sedimentary Research*, 68: 777-787.
- Rothrock, D. A., Yu, Y., and Maykut, G. A., 1999: Thinning of the Arctic sea-ice cover. *Geophysical Research Letters*, 26: 3469-3472.
- Serreze, M. C., Walsh, J. E., Chapin, F. S., III, Osterkamp, T., Dyurgerov, M., Romanovsky, V., Oechel, W. C., Morison, J., Zhang, T., and Barry, R. G., 2000: Observational evidence of recent change in the northern high-latitude environment. *Climatic Change*, 46: 159-207.
- Sharma, G. D., Naidu, A. S., and Hood, D. W., 1972: Bristol Bay: model contemporary graded shelf. *American Association of Petroleum Geologists Bulletin*, 56: 2000-2012.
- Sherwood, C. R., 2000: Numerical model of frazil ice and suspended sediment concentrations and formation of sediment laden ice in the Kara Sea. *Journal of Geophysical Research*, 105: 14061-14080.
- Swan, A. R. H. and Sandilands, M., 1995: *Introduction to Geological Data Analysis*. Malden, MA: Blackwell Science. 446 pp.
- Tucker, W. B., Gow, A. J., Meese, D. A., Bosworth, H. W., and Reimnitz, E. 1999. Physical Characteristics of Summer Sea Ice Across the Arctic Ocean. *Journal of Geophysical Research*, 104:1489-1504.
- Tynan, C. T. and DeMaster, D. P., 1997: Observations and predictions of Arctic climate change: potential effects on marine mammals. *Arctic*, 50: 308-322.
- U.S. Army Coastal Engineering Research Center (CERC), 1984: *Shore Protection Manual*. Vol. 1. 4th ed. Fort Belvoir, VA: U.S. Army Coastal Engineering Center. 603 pp.

Weeks, W. F. and Ackley, S. F., 1986: The growth, structure and properties of sea ice. *In* Untersteiner, N. (ed.), *The Geophysics of Sea Ice*. (NATO ASI B146.) Dordrecht: Martinus Nijhoff, 9-164.

MS submitted December 2001

Site	Year	Location	Length (cm)
1999-1	1999	1	113
2000-1	2000	1	32
2000-2	2000	2	39
2000-3	2000	3	86
2000-4	2000	4	49
2001-1	2001	1	10

TABLE 1. Site designation, year of extraction, location (Figure 1) and core length.



Site	Sediment load of frazil ice layer (g m <sup>-2</sup> )	Resuspension potential
1999-1	59	5.5
2000-1	348	12.6
2000-2	338	12.5
2000-3	384	12.2
2000-4	262	10.2
2001-1	2	-74.7

TABLE 3. Sediment load and resuspension potential for each sampling site.

## Figure captions

FIGURE 1. Sea ice coring locations in Elson Lagoon near Barrow, Alaska. Samples were taken from site 1 in 1999 and 2001, while samples were taken from sites 1 – 4 in 2000. Table 1 lists the corresponding site designations referred to in the text. Bathymetry is in feet.

FIGURE 2. Images of the vertical sea ice structure. These images show the morphology of ice crystals near the top and bottom of core 2000-2 (a-segment 0-5 cm, b-segment 30-35 cm). The thin section images were taken between cross-polarizers. Note the predominance of small, subequant ice crystals in both images and their irregular outlines.

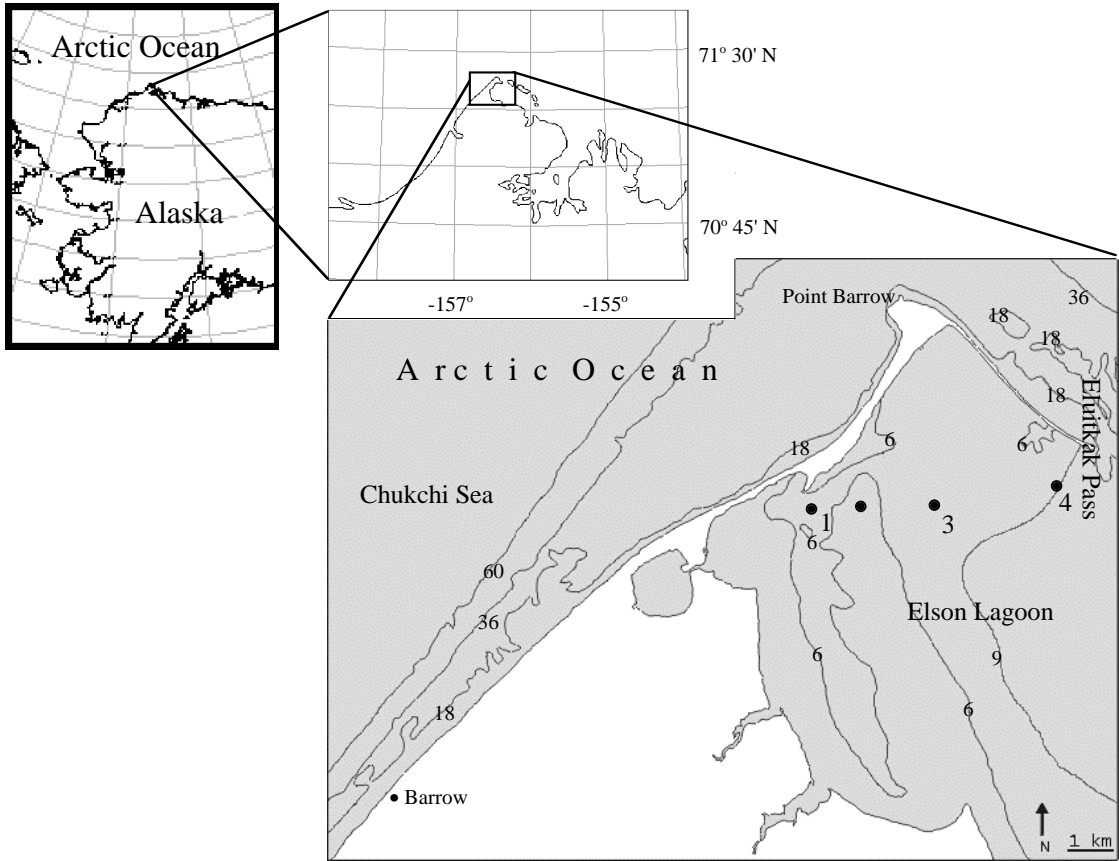
FIGURE 3. A sequence of images showing the spatial distribution of sediment and structural features over a range of scales in sea ice samples acquired in March, 1999. The black marks along the top and left edges of (a) are spaced approximately 10 cm apart. Note meter stick in (b) for scale.

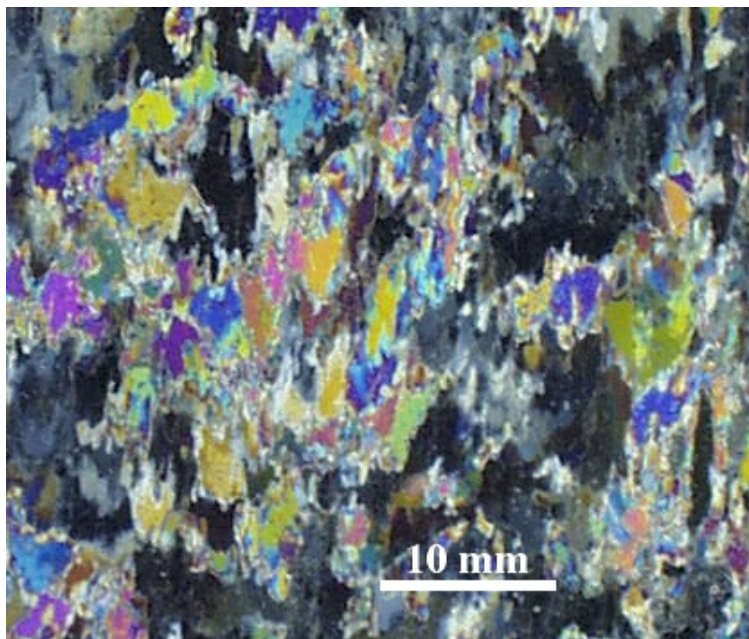
FIGURE 4. Relationships between sediment concentration and mean nearest-neighbor distance and mean aggregate cross-sectional area. The circled data points represent samples 1999-1 (30-40 cm) and 2000-2 (20-30 cm) and were excluded from the regression analysis.

FIGURE 5. Best-fit geometric model relating mean aggregate number density and mean aggregate cross-sectional area to sediment concentration. The circled data points represent samples 1999-1 (30-40 cm) and 2000-2 (20-30 cm) and were excluded from the regression analysis.

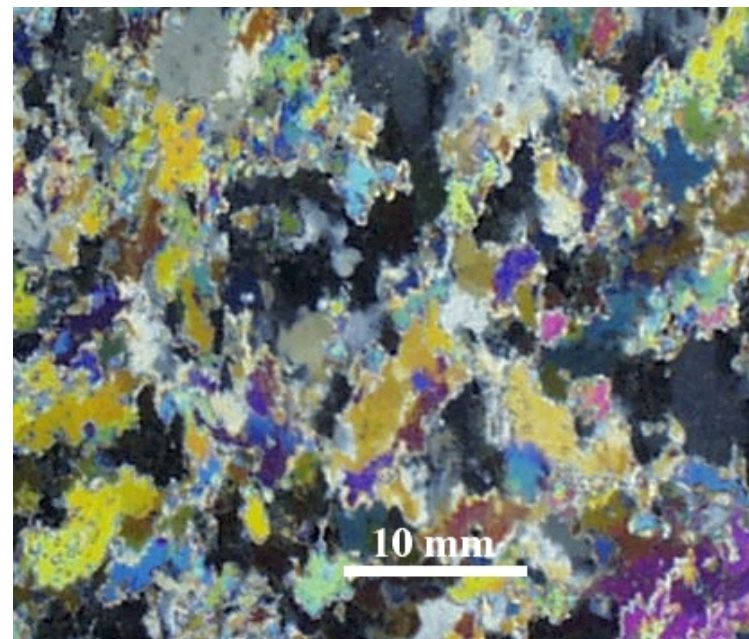
FIGURE 6. Assessment of the resuspension applicability to Elson Lagoon. This chart shows the relationship between AVHRR modified channel 1 percent reflectance and the modeled resuspension potential. Note the increase in percent reflectance values at resuspension potentials greater than  $\sim+5$  (dotted line).

FIGURE 7. Maps of sediment resuspension potential for the 1998, 1999, and 2000 fall freeze-up events. These freeze-up events correspond to the spring 1999, 2000, and 2001 sampling seasons referred to in the text, respectively. Sample sites are the locations indicated on Figure 2 for each of the three sampling seasons. Relative sediment load at each site is indicated by dot size. Wind speed and direction are indicated in the upper left corner of each figure. The contour interval is 2 down to  $-2$ . To enhance readability, below  $-2$  only the  $-10$  contour is marked.





(a)



(b)

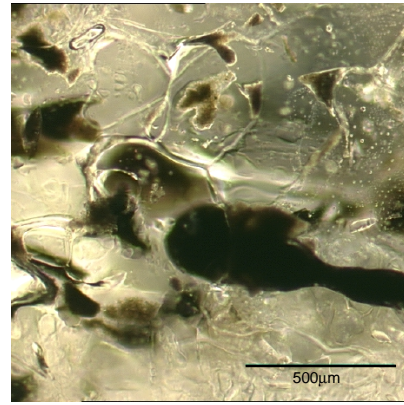
**Figure 2.** Images of the vertical sea ice structure. These images show the morphology of ice crystals near the top and bottom of core 0005-2 (a = segment 0-5 cm, b = segment 30-35 cm). The thin section images were taken between crossed polarizers. Note the predominance of small, subquant ice crystals in both images and their irregular outlines.



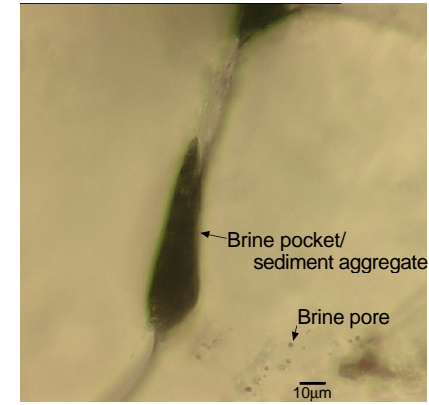
(a)



(b)

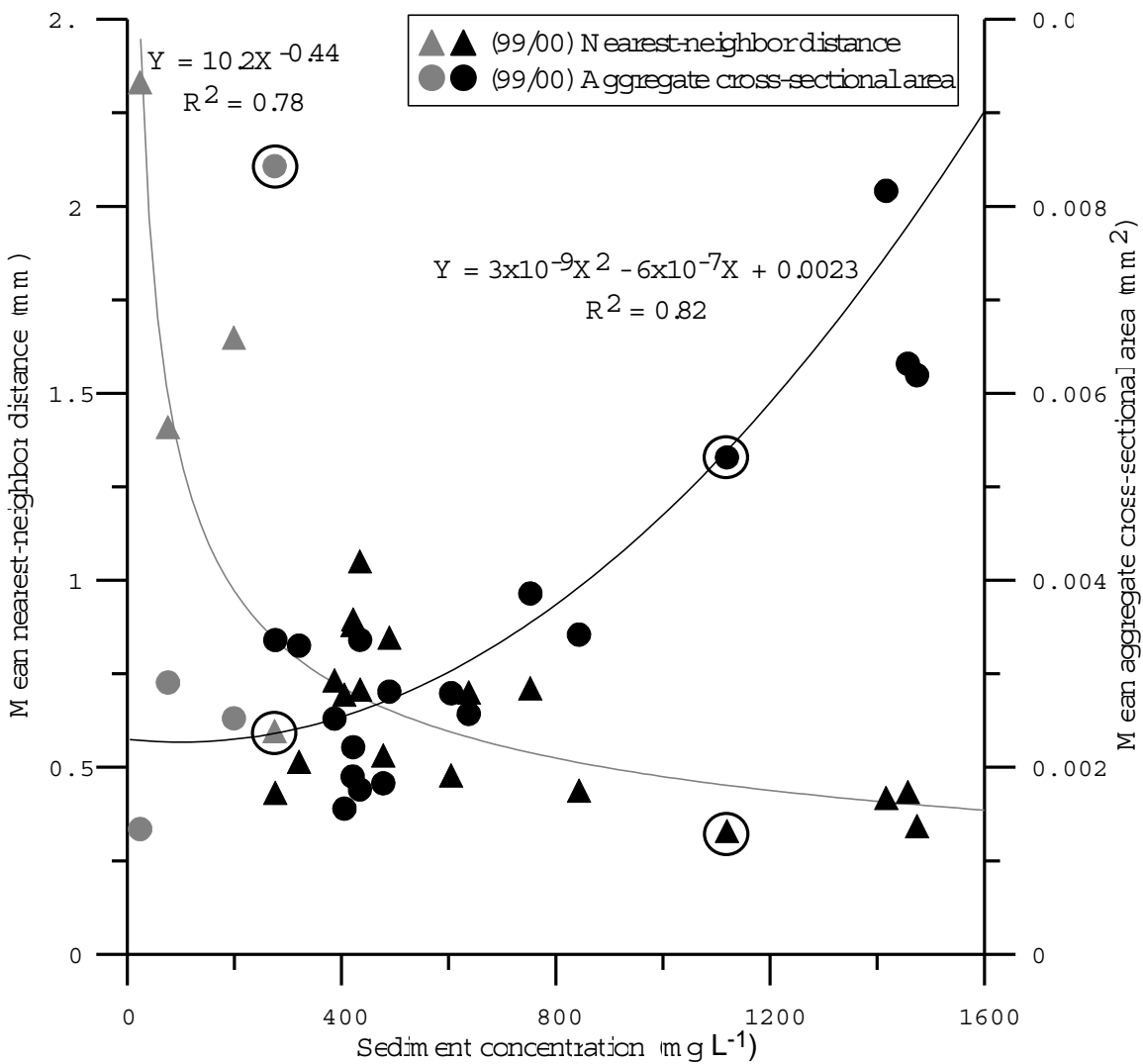


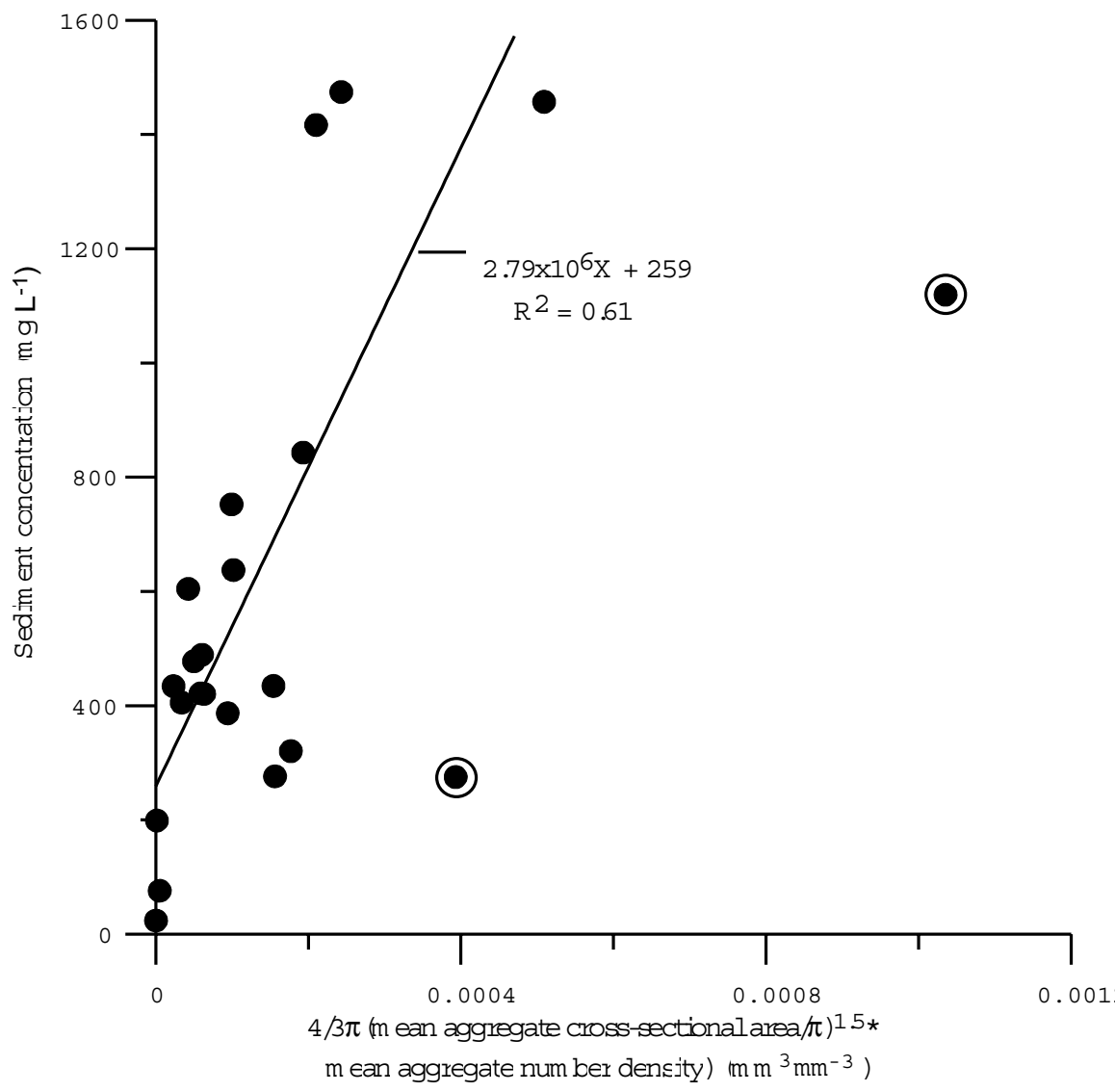
(c)



(d)

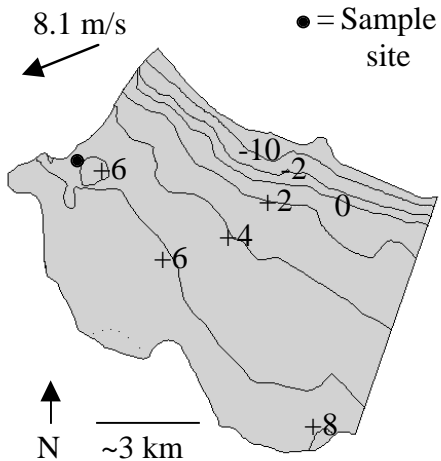
**Figure 3.** A sequence of images showing the spatial distribution of sediment and structural features over a range of scales in sea ice samples acquired in March 1999. The black marks along the top and left edges of (a) are spaced approximately 10 cm apart. Note meter stick in (b) for scale.



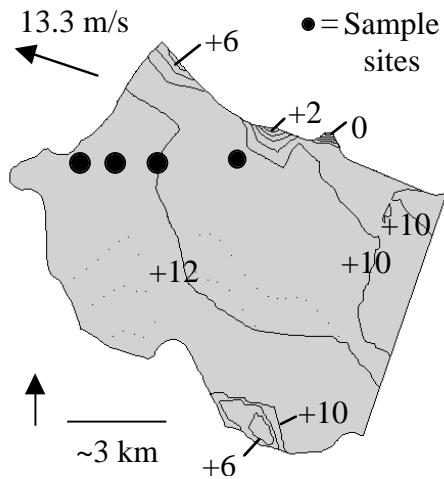




1998



1999



2000

